Journal of Applied Fluid Mechanics, Vol. 16, No. 10, pp. 1887-1900, 2023.
Available online at www.jafmonline.net, ISSN 1735-3572, EISSN 1735-3645.
https://doi.org/10.47176/jafm.16.10.1833

A Simple Design Approach of Two-Phase Ejectors for CO_2 Transcritical Heat Pumps

K. Ameur† and Z. Aidoun

CanmetENERGY, Natural Resources Canada, Varennes, Qc, J3X1S6, Canada

†*Corresponding Author Email: khaled.ameur@NRCan-RNCan.gc.ca*

ABSTRACT

Integrating a two-phase ejector in mechanical vapor compression heat pumps is a practical and low-cost solution for improving performance and reducing energy consumption. Typically, using an ejector to recover part of the important pressure expansion losses in CO_2 systems may improve the operating conditions of the compressor. One of the prerequisites for the success of such an application is the proper design of the ejector. This study is mainly dedicated to developing a simple approach for CO_2 ejector design. The advantage of using the ejector as an expander in a transcritical CO_2 heat pump is first introduced. Compressor operation is particularly improved. The development of an ejector design model for CO_2 expanding from transcritical to two-phase conditions is presented. Validation of the thermodynamic model with experimental results from the literature shows the predictions to be within an acceptable range of discrepancy. The primary nozzle throat diameter calculations do not exceed ±8% of error for transcritical conditions. The error of the predicted pressure at the outlet of the ejector is in the limit of -15% to +3%. A practical design example for estimating the transcritical CO_2 ejectors geometry integrated in a heat pump is presented. The results show the important decrease of primary nozzle diameters with the drop of T_{evap}, especially for the throat. A decrease of D_{mix} also occurs with T_{evap} and an optimal diameter is obtained for each condition considered. The design of the diffuser is based on a compromise between the outlet velocity and the length of the diffuser. The detailed design procedure with the proposed model, complemented with data from the literature, is a valuable tool for rapidly generating useful results and obtaining preliminary designs transcritical CO_2 ejector.

Article History

Received February 22, 2023
Revised May 12, 2023
Accepted May 22, 2023
Available online July 29, 2023

Keywords:

CO_2 transcritical
Ejector design
Expansion-work recovery
Heat pump

1. INTRODUCTION

The climate emergency is a reality that is now well established, due to the increase of greenhouse gases (GHGs) in the atmosphere. The major source of this increase is the energy consumption related to human activity. An important proportion of this consumption is attributed to heating and cooling in the buildings. Indeed, in Canada, greenhouse gas emissions in the building sector in 2020, represents 87.8 Megatonnes of carbon dioxide equivalent (Environment and Climate Change Canada, 2022), right behind oil, gas and transport sectors.

Mechanical vapor compression heat pumps with carbon dioxide (CO_2) as refrigerant represents an attractive solution to energy savings and environmental impact concerns.

Several research studies have explored the potential for enhancing transcritical CO_2 heat pump systems (Sarkar, 2010; Austin & Sumathy, 2011; Ma et al., 2013; Rony et al., 2019). A part of these studies is dedicated to the reduction of the expansion losses through various technologies (Huff & Radermacher, 2003; Saeed et al., 2022). Operating the ejector as an expansion device may offer a practical and low-cost solution for recovering expansion work (Besagni et al., 2016; Aidoun et al., 2019a, b), with the objective of improving heat pump cycles performance.

Kornhauser (1990), is among the first to develop a simplified thermodynamic approach to model the two-phase ejector. A homogeneous and equilibrium two-phase flow model (HEM) was used with the constant pressure concept for the 9mixing process. The motive stream and suction stream reach equal pressure at the inlet of the

NOMENCLATURE

			Greeks
A, a	area, speed of sound	α	void fraction
CFD	Computational fluid dynamics	Δ	difference
COP	Coefficient of performance	η	isentropic efficiency
D	diameter	ρ	density
f	friction factor	φ	angle, efficiency
h	enthalpy	ω	entrainment ratio
IHX	Internal heat exchanger		**Subscripts**
L	length	1	primary inlet
ṁ	mass flow rate	2	secondary inlet
Ma	Mach number	3-8	locations in the ejector
NXP	Nozzle exit position	diff	diffuser
P	pressure	evap	evaporator
Re	Reynolds number	gc	gascooler
s	entropy	isen	isentropic
T	temperature	l	liquid
V	velocity	mix	mixing
X, x	length, vapor quality	t	throat
		v	vapor

constant area mixing section in the ejector. No particular choking conditions were considered for the nozzle. To consider the difference from the theoretical isentropic process, efficiencies were considered for the nozzles and the diffuser. The analysis of a cycle with a compressor and an ejector designed to decrease throttling losses, showed that the improvements in COP, compared to a cycle without an ejector, were significantly affected by the assumed efficiencies.

With a model similar to Kornhauser's, Akagi et al. (2004), investigated the impact of ejector geometry parameters on the transcritical CO_2 refrigeration cycle performance. The results present an improved COP of 11% compared to the basic cycle without ejector. The authors also determined an optimum value for the mixing section diameter. For the considered conditions, the optimum value varied between 2 mm and 2.5 mm. However, a minor variation in the section of less than 1 mm resulted in a significant decline in performance.

Li and Groll (2006), studied theoretically and experimentally a transcritical CO_2 cycle for air-conditioning with an ejector as an expander. The authors considered the Kornhauser model with an empirical correlation to model the diffuser. They also identified an optimal mixing diameter but, in their case, its variation does not rapidly affect the performance. Globally, the results also showed an improved COP of 11% over the cycle without ejector. In a later paper, Liu et al. (2012a) modified the CO_2 ejector model to consider the critical flow based on a two-phase sound velocity calculation. The parametric study showed a very close link between ejector geometry and performance.

Lee et al. (2011) developed another model for CO_2 ejector design, based on the equation of Henry and Fauske (1971) to evaluate the critical mass flux. Thermal non-equilibrium effects were introduced through empirical parameters. The designed ejector was tested in an air-conditioning system; at equivalent operating conditions, the COP was roughly 15% greater compared to the conventional system. Results showed the existence of optimal design parameters for each test condition. In their study, Zha et al. (2007) compared two approaches to evaluate the critical flow in the nozzle. One based on Henry and Fauske equation and the other on a sound velocity calculation by a physical method. The predicted flow rate with physical model is relatively close to the experimental results.

Ameur et al. (2016) and Ameur & Aidoun (2021) in their model of the two-phase ejector evaluated the critical conditions in the nozzle by adjusting the outlet pressure until the mass flux is maximized. This homogeneous approach eliminates the need for calculating the sound velocity in the two-phase flow stream. Transcritical CO_2 heat pump cycle simulations demonstrate an advantage in terms of COP and heating capacity at low evaporator temperatures when utilizing the ejector. At the lowest evaporator temperature considered, gas cooler capacity, evaporator capacity and the COP improved by 14%, 23% and 9% respectively. The results also indicated the necessity to adjust the ejector's geometry to accommodate capacity changes.

The review of Ringstad et al. (2020) provided a thorough assessment of the recent advancements of two-phase CO_2 ejector modeling. The review focused especially on the CFD approach such as multiphase and turbulence modeling. The review showed that the HEM model could attain a satisfactory level of precision under supercritical conditions. At low-pressure motive conditions, the accuracy quickly drops due to non-equilibrium expansion. The CFD approach, with its ability to analyze the internal details of the ejector flow, is well suited for design optimization. However, it remains complex and costly to implement.

The literature clearly shows the energy benefit of integrating a two-phase ejector in transcritical CO_2 vapor compression systems. However, a high sensitivity of the system performance with respect to the ejector's geometry is observed. Thus, the design of the ejector becomes a

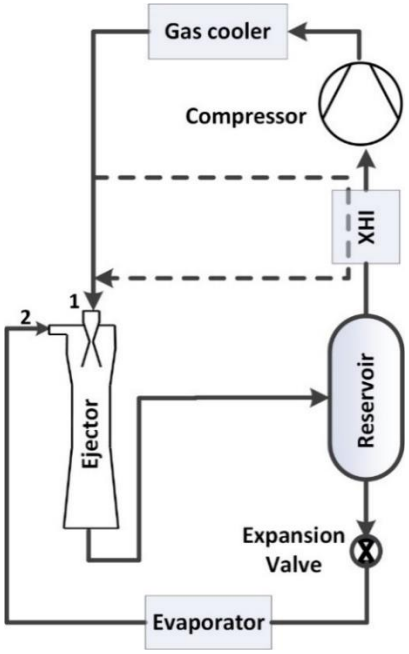

Fig. 1 A transcritical CO_2 heat pump with an ejector as an expansion device

crucial step in the use of such systems. In this paper, a detailed modeling procedure is presented for this purpose.

In this development, the first section shows theoretical results that highlight the benefits of incorporating an ejector in the heat pump. The rest of the article is dedicated to ejector design. The model is based on a relatively simple and robust thermodynamic approach, with reasonable accuracy under supercritical nozzle inlet conditions. Choking in the motive nozzle is considered through a mass flux maximization method. For the secondary nozzle calculation, a fixed Mach number is achieved by adjusting the mass flux. Modeling of the mixing process is considered in two steps, with variable pressure unlike the common approach. The converging zone of the mixing chamber and the remaining zone with constant cross-section are considered separately. Finally, after exhaustive validations with experimental data, the model is applied to design ejectors for a CO_2 transcritical heat pump with different conditions at the heat source. The proposed thermodynamic design model is complemented with the use of data from the literature to provide all the necessary geometrical aspects of the ejector. The model provides the necessary support for the design stage of any CO_2 transcritical two-phase ejector application. It is a valuable tool for rapidly generating useful data and obtaining preliminary designs.

2. EJECTOR ROLE IN HEAT PUMP APPLICATION

The application of the ejector considered in this study is depicted in Fig. 1. It is a transcritical CO_2 heat pump cycle with a two-phase ejector to recover a part of the throttling losses due to the expansion. In this ejector application, compared to the conventional mechanical vapor-compression system, almost the entire expansion process takes place in an ejector instead of an isenthalpic valve.

The motive fluid for the ejector primary nozzle is the high-pressure CO_2 stream flowing the gas cooler. The mixture leaving the ejector collects in the reservoir (separator). The evaporator is supplied with liquid from the reservoir, and the vapor produced is then directed to the secondary inlet of the ejector. The remaining saturated vapor in the reservoir is directed to the compressor suction. The necessary superheating at the compressor suction is achieved by means of an internal heat exchanger.

Note that for this type of cycle, the entrainment of the ejector should present a particular value to maintain stable conditions during the cycle's operation. It is important to have the appropriate value of the quality at the ejector outlet, to meet the mass balance constraint in the reservoir.

The theoretical results shown in Fig. 2-3, related to the ejector contribution in a transcritical CO_2 heat pump, are based on models developed in a previous study (Ameur & Aidoun, 2021). For each simulated evaporator condition, the heat rejection pressure and the ejector entrainment are adjusted to their optimal values. The gas cooler outlet temperature is maintained constant at 35 °C.

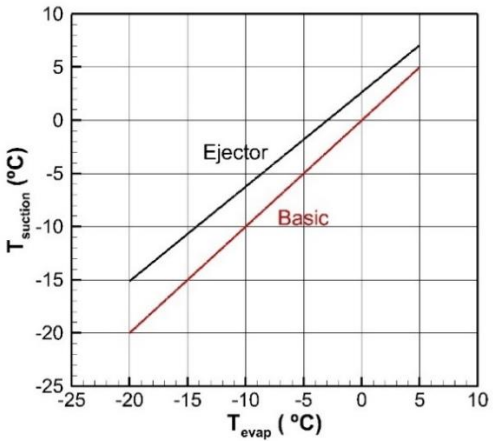

Fig. 2 Improvement of the compressor suction by using an ejector in the cycle

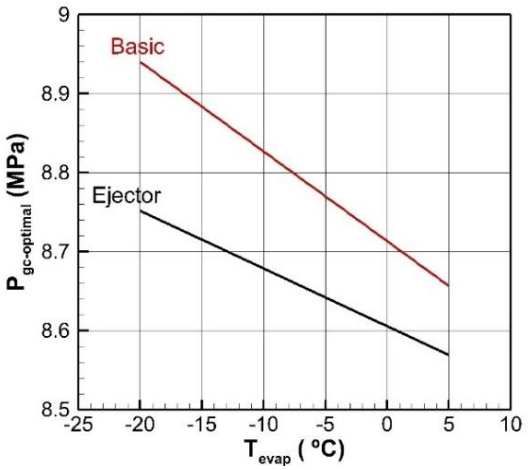

Fig. 3 Ejector impact on the optimal gas cooler pressure

Figure 2 presents the improvement of the compressor suction condition by using a transcritical CO_2 ejector. The recovered work by the ejector contributes to compress partially the vapor leaving the evaporator and improves the operating conditions of the compressor.

The presence of an ejector in the cycle leads to a higher saturation temperature at the compressor inlet than the basic configuration without an ejector. This trend is more pronounced for low evaporator temperatures where the potential for energy recovery is greater. Another useful impact of the ejector is a relative decrease of the optimal gas cooler pressure (Fig. 3), which helps to reduce the compression ratio.

The integration of an ejector in a heat pump as an expansion device can enhance the operation of the compressor, resulting in a positive impact on the overall system performance. In addition, the compressor shutdown for cold weather conditions could be delayed due to higher suction temperature.

3. EJECTOR DESIGN MODEL

The model developed to design the two-phase CO_2 transcritical ejector relies on a thermodynamic approach. It is quite similar to the one developed for the performance evaluation, described in a previous paper (Ameur & Aidoun, 2021). However, in the present version, particular attention is devoted to the ejector geometry, with more appropriate handling of the mixing zone for more realistic design aspects such as the consideration of the wall friction to control the length of this zone. The different internal sections of the ejector considered in the modeling are shown in Fig. 4.

The thermodynamic methodology is mainly based on the conservation law and on approximations that make it relatively simple and generates results rapidly. Steady-state and one-dimensional variation in the flow direction are assumed. The other assumptions (Ameur et al., 2016; Takleh & Zare, 2019) used in the present model are:

- HEM is considered for the two-phase flow aspects.
- The nozzles and the diffuser losses are considered through isentropic efficiencies.
- Flow in the nozzles is considered choked.
- In the mixing convergent zone, a coefficient is added to momentum equation to consider losses due to the mixing process of the primary and secondary flow.
- In the mixing zone with constant cross-section, pressure losses are considered through a wall friction calculation.

3.1 Methodology

The main equations used in the ejector design calculations are the integral form of the conservation law of mass, momentum and energy. Balances are applied to the different considered sections of the ejector (Fig. 4), proceeding from the inlets to the outlet, according to the following order:

1. Primary nozzle convergent (1-3).

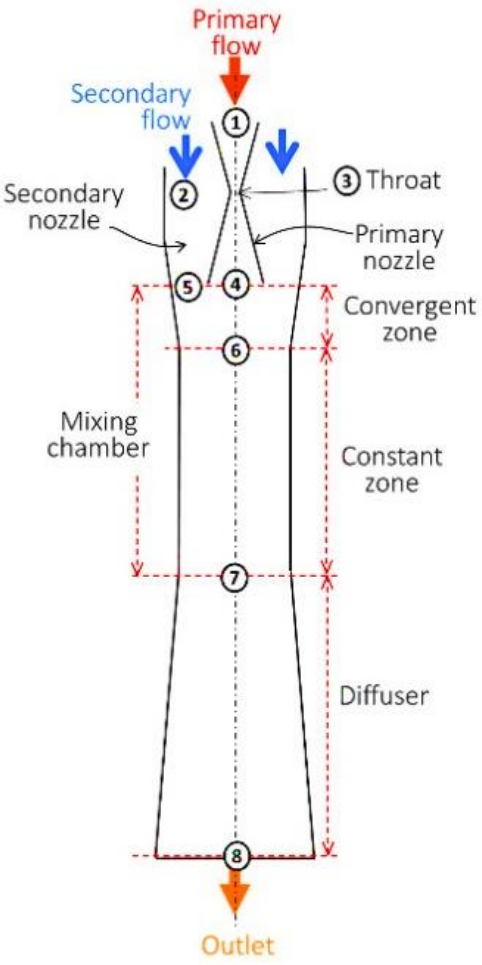

Fig. 4 Internal geometric sections of the ejector

2. Secondary nozzle (2-5).
3. Primary nozzle divergent (3-4).
4. Mixing convergent zone (4-5 to 6).
5. Mixing constant zone (6-7).
6. Diffuser (7-8).

The NIST-REFPROP database equations (NIST, 2010) are integrated to the model to assess the CO_2 thermophysical properties. The conditions imposed at the ejector inlets allow the calculation initialization. The various flow parameters such as area, enthalpy, pressure, quality, velocity, etc., are evaluated at the limits of the different ejector sections. Details of the overall calculations are summarized below.

Primary nozzle

The primary nozzle (Fig. 4) presents a convergent (1-3) and a divergent (3-4), allowing the expansion of the transcritical CO_2 by accelerating the flow.

The primary nozzle is assumed to be in choking conditions. The calculation is carried out by adjusting the mass flux at the throat nozzle to the maximum (Ameur et al., 2016; Taslimi Taleghani et al., 2018). This approach eliminates the need to calculate the speed of sound in two-phase flow conditions, which can be challenging.

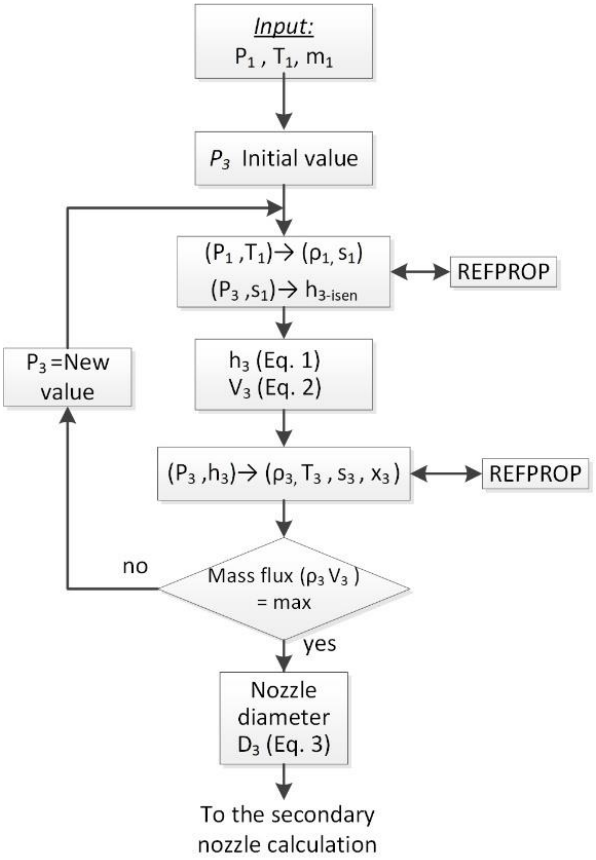

Fig. 5 Main steps calculations of the throat diameter

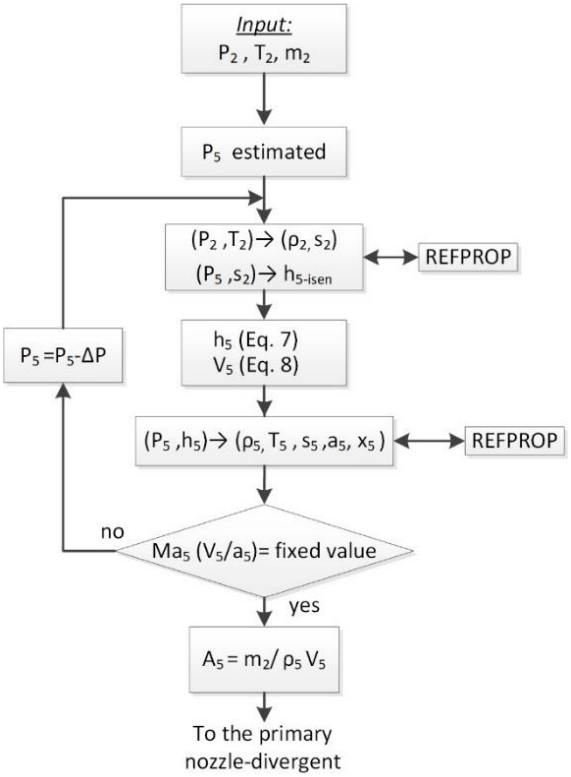

Fig. 6 Secondary nozzle calculations

The flowchart of Fig. 5 summarizes the main calculation steps of primary nozzle throat. An iterative process on the pressure at the throat (P_3) is carried out until obtaining a maximum value of the mass flux ($\rho_3 V_3$).

The enthalpy at the throat is evaluated based on an isentropic efficiency (η_{prim1}) (Eq. (1)). The throat velocity (V_3) is estimated through energy conservation (Eq. (2)).

$$h_3 = h_1 - \eta_{prim1}(h_1 - h_{3-isen}) \quad (1)$$

$$V_3 = \sqrt{2(h_1 - h_3)} \quad (2)$$

When the maximum flux is reached, the conservation equation of mass is applied to calculate the throat area and the corresponding diameter (Eq. (3)).

$$D_3 = \sqrt{\frac{4\,\dot{m}_1}{\pi\,\rho_3 V_3}} \quad (3)$$

The divergent of the primary nozzle allows for a higher expansion with the possibility to accelerate the flow to supersonic speed. The calculation structure of this zone requires no iterative process. It is initialized by the knowledge of the conditions at the throat and the outlet pressure of the divergent (P_4) must also be known.

By means of an isentropic efficiency (η_{prim2}), the enthalpy at the outlet of the primary nozzle (h_4) is estimated with Eq. (4). The velocity at the primary nozzle outlet is calculated with Eq. (5) which represent energy conservation between the throat and the outlet.

$$h_4 = h_3 - \eta_{prim2}(h_3 - h_{4-isen}) \quad (4)$$

$$V_4 = \sqrt{2(h_3 - h_4)} \quad (5)$$

Finally, the mass balance enables to evaluate the outlet area and the related diameter (Eq. (6)).

$$D_4 = \sqrt{\frac{4\,\dot{m}_1}{\pi\,\rho_4 V_4}} \quad (6)$$

Secondary nozzle

The convergent area surrounding the primary nozzle upstream of the mixing chamber, internal zone (2-5) in Fig. 4, is referred to as the secondary nozzle. This area is considered as the place where the secondary flow starts to be driven while undergoing expansion. The estimation of this expansion is based on a mass flux calculation until reaching a desired Mach number. It is supposed that the vapor undergoing low expansion in the secondary nozzle does not experience any condensation. Thus, simplifying the speed of sound evaluation. For design conditions, the Mach number is selected theoretically close to sonic velocity. However, note that in various CFD studies, only a subsonic flow is detected inside the secondary nozzle (Zhu & Jiang, 2018; Giacomelli et al., 2019), and only further downstream, inside the mixing zone that Mach number exceeds the critical condition.

Figure 6 shows a summary of the main calculations of the secondary nozzle convergent. The output pressure (P_5) is reduced until Ma_5 reaches the selected value. The speed of sound (a_5) is estimated by REFPROP using a single-phase formulation. Considering efficiency (η_{sec}) for the expansion, the enthalpy at the secondary nozzle outlet (h_5)

is estimated with Eq. (7). Conservation of the energy applied to the secondary nozzle (Eq. (8)) allows the estimation of the outlet velocity (V_5).

$$h_5 = h_2 - \eta_{sec}(h_2 - h_{5-isen}) \quad (7)$$

$$V_5 = \sqrt{2(h_2 - h_5)} \quad (8)$$

At the end, the mass balance is used to estimate the outlet area.

Mixing chamber

The mixing chamber refers to the section between the outlet of the primary nozzle and the inlet of the diffuser (see Fig. 4). The modeling of this part of the ejector is considered in two steps. First, the flows exiting the nozzles mix in the convergent zone. Then the mixing process continues in the constant zone. In the present model, the mixing differs with the common approach (Kornhauser, 1990) by assuming the process to develop with variable pressure.

Mixing convergent zone

The main steps of calculation of the mixing convergent zone are summarized in the flowchart of Fig. 7. The output area of this section (A_6) is an input, since the diameter of the mixing constant zone (D_6=D_{mix}) is imposed. The selection of the optimal D_{mix} is presented in section 4.2 where a typical example of an ejector design is detailed.

The exit velocity (V_6) is adjusted until the conservation of the mass at the exit of this zone is achieved. Pressure and enthalpy are adjusted as follows:

Losses due to mixing are introduced in the conservation equation of momentum (Eq. (9)), through the coefficient (φ_{mix}) (Eames et al., 1995):

$$(P_4A_4 + P_5A_5) + \varphi_{mix}(\dot{m}_1V_4 + \dot{m}_2V_5) = P_6A_6 + \dot{m}_6V_6 \quad (9)$$

Pressure at the outlet of the mixing convergent zone is estimated with Eq. (9) combined to the mass conservation equation,

$$P_6 = [(P_4A_4 + P_5A_5) + \varphi_{mix}(\dot{m}_1V_4 + \dot{m}_2V_5) - (\dot{m}_1 + \dot{m}_2)V_6]A_6^{-1} \quad (10)$$

Based on the conservation of energy, the enthalpy at the outlet of the mixing convergent zone is estimated as,

$$h_6 = \frac{1}{1+\omega}\left(h_4 + \frac{V_4^2}{2}\right) + \frac{\omega}{1+\omega}\left(h_5 + \frac{V_5^2}{2}\right) - \frac{V_6^2}{2} \quad (11)$$

ω is the entrainment ratio (secondary mass flow rate to primary mass flow rate).

Mixing constant zone

Modeling of the mixing zone with constant cross-section evolves an iterative calculation of the outlet velocity (V_7). The main steps of calculations are summarized in the flowchart of Fig. 8.

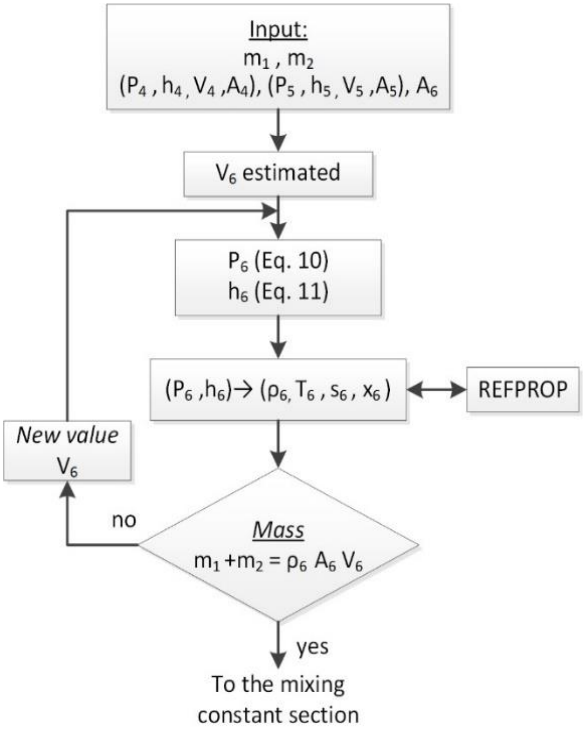

Fig. 7 Mixing convergent zone calculations

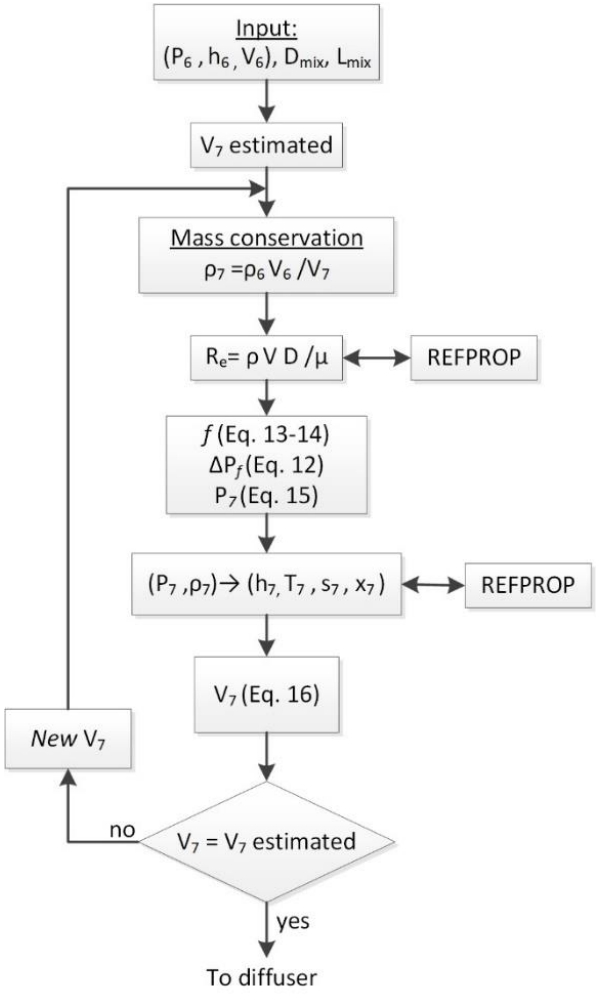

Fig. 8 Mixing constant zone calculations

To control the length (L_{mix}) of this zone, the wall friction is introduced in the momentum equation. The Darcy relation evaluates the pressure loss, due to friction according to the homogeneous model,

$$\Delta P_f = \frac{1}{2} f \frac{(\rho V)^2 L_{mix}}{\rho D_{mix}} \quad (12)$$

The friction factor f is evaluated with Eq. (13) and Eq. (14) depending on the Reynolds number (Aakenes, 2012). For Re < 2000 (laminar flow),

$$f = \frac{64}{R_e} \quad (13)$$

For Re ≥ 2000 (turbulent flow),

$$\frac{1}{\sqrt{f}} = 2\,\mathrm{Log}\left(R_e \sqrt{f}\right) - 0.8 \quad (14)$$

The pressure at the outlet of the mixing constant zone is determined using the momentum equation,

$$P_7 = P_6 + \rho_6 V_6^2 - \rho_7 V_7^2 - \Delta P_f \quad (15)$$

The flow velocity is estimated using the energy equation,

$$V_7 = \sqrt{2(h_6 - h_7) + V_6^2} \quad (16)$$

Finally, the iterative calculations are stopped when the estimated and calculated velocities are converging.

Diffuser

The compression process of the diffuser is mainly assessed with energy and mass equations. The calculations are stopped once the flow decelerates until a selected outlet velocity. The main steps of the diffuser evaluation are as follows:

With setting a diffuser efficiency (η_{diff}), enthalpy at the ejector outlet is estimated with Eq. (17).

$$h_8 = h_7 + \frac{h_{8-isen} - h_7}{\eta_{diff}} \quad (17)$$

The enthalpy h_{8-isen} is estimated using REFPROP since P_8 and s_7 are known.

Ejector outlet velocity is assessed with the energy equation,

$$V_8 = \sqrt{2(h_7 - h_8) + V_7^2} \quad (18)$$

Finally, after convergence of the calculations, the mass balance enables to evaluate the outlet diameter,

$$D_8 = \sqrt{\frac{4(\dot{m}_1 + \dot{m}_2)}{\pi \rho_8 V_8}} \quad (19)$$

3.2 Model Validation

The two-phase CO_2 ejector design model is validated through the nozzle throat diameter and the outlet pressure of the ejector. The experimental data used in this section come from the literature. Note that the studies used to validate the throat diameter are more abundant than those related to the pressure outlet. The nozzle throat validation requires only the knowledge of the conditions at the primary inlet and the throat diameter, unlike the pressure validation which requires more details on the geometry of the entire ejector.

The modeling error is mainly evaluated by the relative difference,

$$\Delta Y = \frac{Y_{experiment} - Y_{model}}{Y_{experiment}} \times 100\% \quad (20)$$

The Y variable can be either the throat diameter or the outlet pressure.

In the literature, thermodynamic two-phase ejector studies recommend different efficiencies values. According to literature recommendations and some further calculation refinements, the efficiencies used in this study are: 0.9, 0.85, 0.8 for nozzles, mixing and diffuser respectively.

3.2.1 Throat Diameter

More than 155 experiment points from nine studies (Akagi et al., 2004, 2008; Banasiak & Hafner, 2013; Smolka et al., 2013; Banasiak et al., 2014; Palacz et al., 2017; Zhu et al., 2017; Giacomelli et al., 2019; Mastrowski et al., 2019) are used in Fig. 9-10 to validate the CO_2 ejector throat diameter calculations. These experimental data cover a wide range of conditions at the ejector inlet. Pressures and temperatures at the primary inlet (P_1=54-105 bar, T_1=10-45 ºC) represent liquid, sub-critical and supercritical conditions.

Figures 9 and 10 show the calculation error on the throat diameter (ΔD_t) according to various pressure and temperature at the primary nozzle inlet. Globally, the margin of error is less ±8% for transcritical condition (P>73.7 bar and T>30.9 ºC). For the subcritical conditions, it could reach ±25%.

Most likely this discrepancy is related to the inadequacy of the two-phase homogenous equilibrium model under subcritical conditions. Palacz et al. (2017) showed in their study that for nozzle inlet conditions

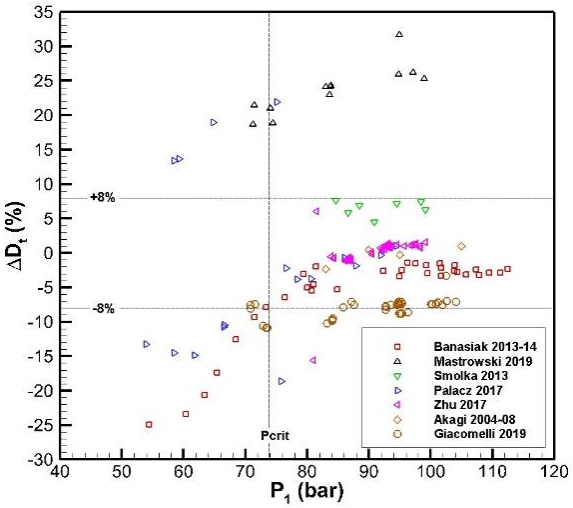

Fig. 9 Throat diameter error distribution with the primary pressure

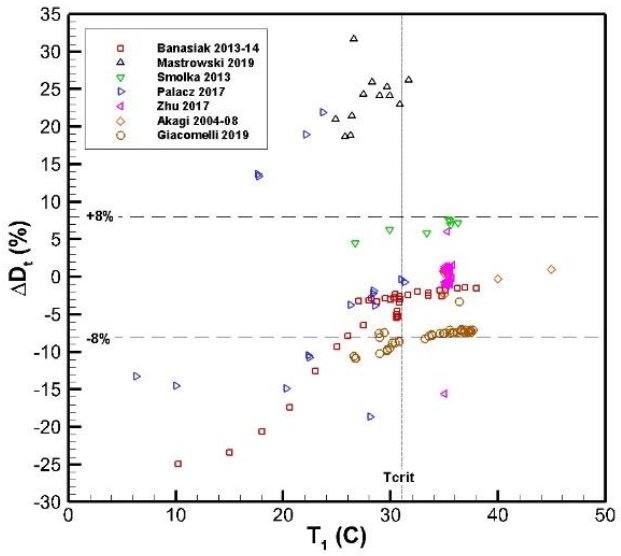

Fig. 10 Throat diameter error distribution with the primary temperature

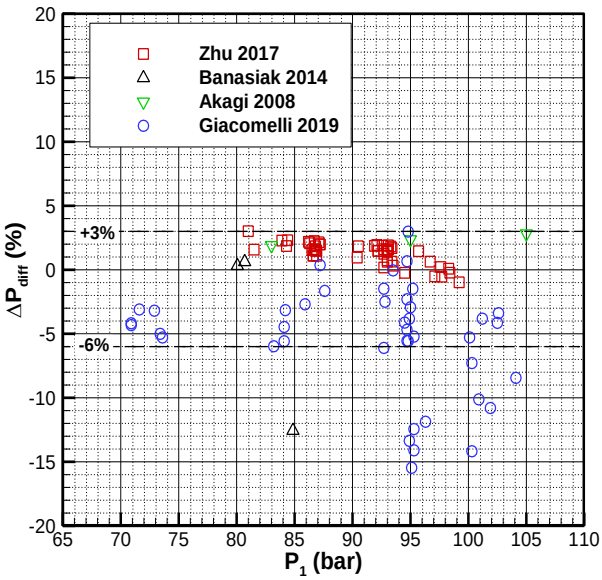

Fig. 11 Ejector outlet pressure error distribution with the primary pressure

below the critical points, the metastability phenomenon exerts a more significant influence. The authors were able to improve the accuracy of the homogeneous equilibrium model by considering a relaxation time formulation to reflect the delayed evaporation in the nozzle for the lower temperature and pressure. Two other metrics are also calculated for this validation: the root mean square error (RMSE) and the normalized root mean square error (NRMSE). In transcritical conditions, RMSE is 0.055 mm and NRMSE is 9.1% which is in line with the above analysis.

3.2.2 Outlet Pressure

A part of the experimental data used in the throat diameter validation (Akagi et al., 2008; Banasiak et al., 2014; Zhu et al., 2017; Giacomelli et al., 2019) is selected to validate the entire ejector. Table 1 summarizes this data used as input for the model.

Table 1 Experimental data used in ejector validation

Authors	Akagi et al. (2008)	Banasiak et al. (2014)	Zhu et al. (2017)	Giacomelli et al. (2019)
#Points	3	3	51	42
P_1 (bar)	83-105	80-85	81-99	71-104
T_1 (°C)	35-45	29-35	34-36	26-38
P_2 (bar)	45	35.5	29-36	24-39.4
T_2 (°C)	12	5-29	20-24	5.8-22
ω	0.4-0.5	0.4-0.6	0.1-0.8	0.1-0.57
D_{mix} (mm)	2	2-5	2	2
L_{mix} (mm)	23	15-50	18	16.9

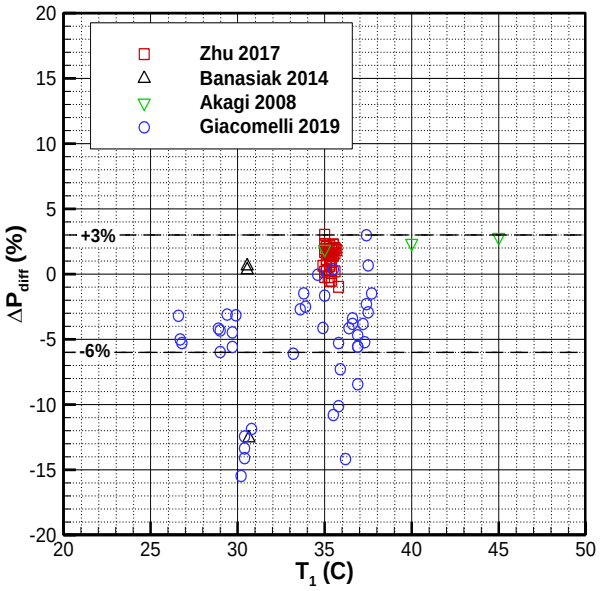

Fig. 12 Ejector outlet pressure error distribution with the primary temperature

Figures 11 and 12 show the error introduced by the model prediction on the ejector outlet pressure (ΔP_{diff}), according to the primary pressure and temperature respectively. A maximum error of -16% is recorded, however a large number (≈88%) of calculations are in the range of -6% to +3%. The RMSE and NRMSE are equal to 1.8 bar and 7.8% respectively.

The observations above show that the model developed for the transcritical CO_2 ejector offers acceptable design predictions.

A basic use of the ejector design model allows to deduce the main diameters and the length of the mixing constant zone. In the next sections, a typical ejector design example with more details of the geometry is presented. The conditions surrounding the ejector are derived from the projected application.

4. DESIGN FOR A HEAT PUMP APPLICATION

A practical example of ejector design for heat pump application is presented in this section. The design conditions of the cycle are first identified. The next step is to use the developed model to estimate the ejector geometry. As the model does not evaluate the complete details of the ejector, data from the literature are used to overcome these limitations. The details of this interaction between the model and literature data are presented below.

4.1 Design Conditions

The design conditions are evaluated based on a previous calculation of a transcritical CO_2 heat pump with an ejector as an expansion device (Ameur & Aidoun, 2021). The cycle model was developed within the context of a test bench project. The heating capacities considered do not exceed 11 kW under the most favorable conditions.

The thermodynamic cycle model is essentially built on the conservation law of mass and energy. A transcritical CO_2 semi-hermetic reciprocating compressor was used in the model, through correlations provided by the manufacturer (Bitzer, Model 2MTEK). The simple ejector model employed along with the procedure for performance evaluation in the cycle does not handle the design details. The compressor frequency was set to 35 Hz with 10 K as superheat at the suction. A temperature of 35 °C was selected for the refrigerant at the gas cooler outlet. These working conditions are the same as those used in Fig. 2 and 3 to show the advantage of using an ejector as an expander.

Table 2 summarizes the main design conditions of the ejector. They correspond to different temperatures at the evaporator. The high-pressure activation (P_1) is set for maximum COP which corresponds to the optimal gas cooler pressure. The entrainment ratio is that which achieves mass balance in the separator. A small superheat is imposed at the ejector secondary inlet.

4.2 Design Approach

At the stage of ejector manufacturing, the main geometry parameters in Fig. 13 need to be known.

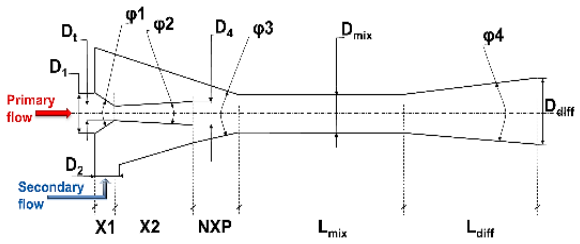

Fig. 13 Geometry parameters of an ejector

Overall, diameters are estimated by the design model presented above. D_1 and D_2 diameters of the primary and secondary inlets are easily evaluated based on an estimation of the inlet velocity since the fluid conditions are known.

The different angles (φ) are selected based on data found in the literature as reported in Table 3, which summarizes some CO_2 ejector geometry characteristics.

The references related to Table 3 (Akagi et al., 2008; Elbel & Hrnjak, 2008; Banasiak & Hafner, 2011; Elbel, 2011; Nakagawa et al., 2011; Banasiak et al., 2012; Bouziane et al., 2012; Lucas and Koehler, 2012; Liu et al., 2012b; Minetto et al., 2012; Banasiak et al., 2015; Palacz et al., 2017; Zhu et al., 2017) are mostly experimental and some CFD studies are also included. The last column of the table shows optimal value after several tests, or simply a value that more frequently appears in the literature.

The lengths X1, X2 and L_{diff} are evaluated with the calculated diameters and the imposed angles. The NXP length is assumed as $3D_{mix}$ (Table 3) but since this length is a parameter that depends greatly on the conditions and the geometry, it is recommended, when testing, to have a nozzle displacement device.

As shown in the flowchart of Fig. 14, the ejector design model is used iteratively on the diameter and length of the mixing zone. The iterative calculation on D_{mix} is stopped when the ejector outlet pressure is maximum. On the other hand, the model does not allow to show an optimal pressure with the variation of L_{mix}, in this case

Table 2 Design conditions

T_{evap} (°C)	5	0	-5	-10	-15	-20
P_1 (bar)	85.5	86.2	86.6	86.9	87.2	87.5
T_1 (°C)	31.9	32.1	32.3	32.5	32.6	32.7
m_1 (g/s)	56.4	47.9	40.5	34	28.4	23.5
P_2 (bar)	39.7	34.8	30.4	26.5	22.9	19.7
T_2 (°C)	7	2	-3	-8	-13	-18
m_2 (g/s)	36.3	29.6	23.9	19.4	15.7	12.6
ω	0.64	0.62	0.59	0.57	0.55	0.53

Table 3 Geometry parameters of CO_2 ejectors

Parameters		Tested range	Selected value
Primary nozzle	φ1	30°	30°
	φ2	0-5°	2°
	$(D_4/D_t)^2$	1-1.52	1.25
Mixing	NXP	(0.55-6)D_{mix}	$3D_{mix}$
	φ3	42°, 45°	45°
	L_{mix}/D_{mix}	2-29.4	6-10
	$(D_{mix}/D_t)^2$	2-37	5-11
Diffuser	φ4	5-15°	5°
	D_{diff}/D_{mix}	1.2-5	3.3

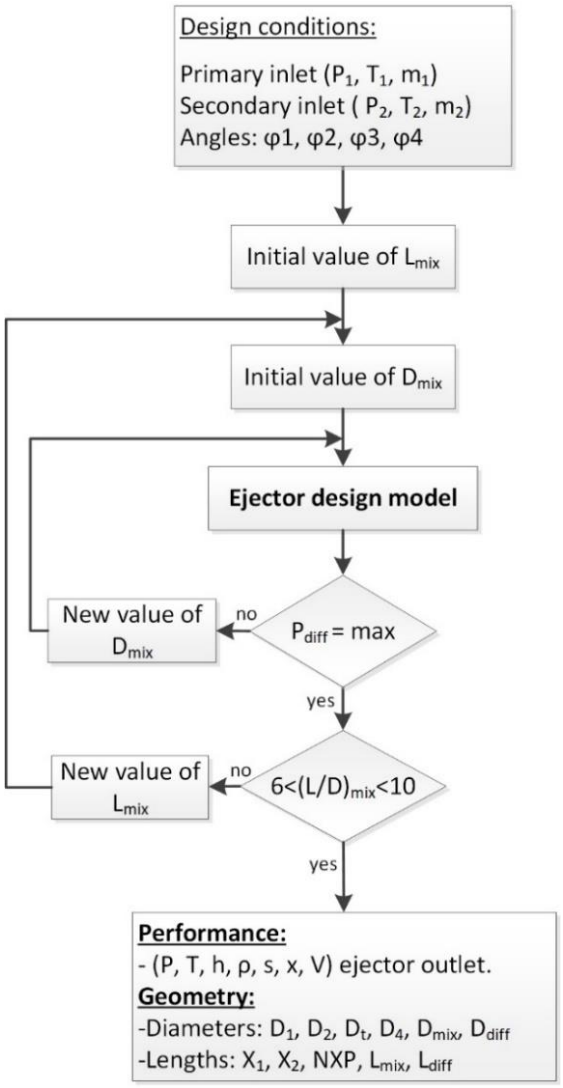

Fig. 14 Flowchart of an ejector design approach

iterative calculations are stopped when the ratio L_{mix}/D_{mix} is in the range of 6-10 (Table 3).

The design details of the ejectors with the conditions of Table 2 are presented below.

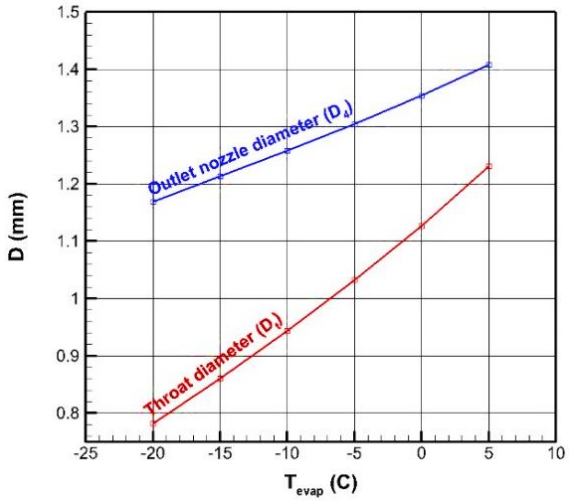

Fig. 15 Throat diameter and outlet primary nozzle diameter for different T_{evap}

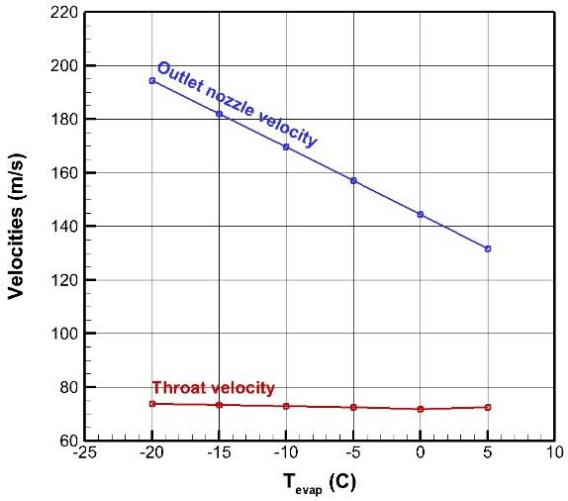

Fig 16. Velocity at primary nozzle's throat and outlet for different T_{evap}

Primary nozzle diameters

Figure 15 shows the throat (D_t) and the nozzle outlet (D_4) diameters variation for different evaporator temperature. The two diameters decrease with T_{evap}, with a steeper slope for the variation of the throat diameter than outlet nozzle diameter.

As the conditions of the primary nozzle inlet present small variations with T_{evap} (see Table 2), the choking at the throat is established nearly in the same way. Thus, the change in throat diameter follows principally the drop of the primary flow feeding the nozzle, which is mainly affected by the decrease of the gas cooler capacity with T_{evap}. The primary nozzle outlet diameter is more associated with the pressure of the secondary flow, which decreases with the drop of T_{evap}. Thus, a greater expansion is necessary in the nozzle divergent to match lower evaporator temperatures.

Flow velocities at the throat and at the outlet of the primary nozzle are reported in Fig. 16 for different T_{evap}.

Throat velocity is almost constant and confirms the previous comment that choking conditions at the throat depend essentially on the nozzle inlet conditions, which in this case almost do not vary. The primary nozzle outlet velocity increases with decreasing T_{evap}, which is an expected trend with the necessary higher expansion in the nozzle divergent to match lower evaporator temperature conditions.

At T_{evap}=5 ºC, the velocities at the throat and at the outlet nozzle are 72 m/s and 131 m/s respectively. The order of magnitude of these values agree with those calculated by Smolka et al. (2013) who used a CFD approach to simulate a CO_2 ejector at slightly different conditions.

Note that a calculation of the throat Mach number with throat velocities of Fig. 16, and the speed of sound estimated by Wood's relation (Cardemil & Colle, 2011) (Eq. (21)), gives a subsonic value of the Mach number (0.31).

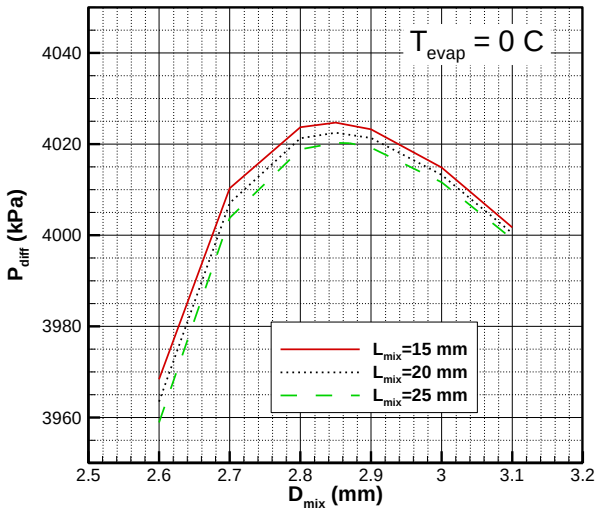

Fig. 17 Variation of ejector pressure outlet with D_{mix} and L_{mix} for T_{evap}=0 ºC

$$a^2 = \frac{1}{\rho}\frac{1}{\left(\frac{\alpha}{\rho_v a_v^2} + \frac{1-\alpha}{\rho_l a_l^2}\right)} \quad (21)$$

In the CFD calculations of Giacomelli et al. (2019) two other different sound speed formulations (Wallis and Brennen equations) were used to evaluate the Mach number. Neither of the two shows a sonic line in the throat (Ma<0.5). Clearly, this low Mach number values represent an approximation because the primary nozzle is choked with the considered conditions. Assessing the speed of sound at the throat, where the flow quality is very low, may present significant uncertainty (Ameur et al., 2016).

Mixing chamber geometry

The selection of D_{mix} is achieved by maximizing the outlet pressure of the ejector (P_{diff}) as seen in Fig. 17 for T_{evap}=0 ºC. For a given length L_{mix}, the increase of D_{mix} is associated with a rise of the P_{diff} up to an optimal value of the diameter which corresponds to a maximum pressure. Beyond the optimal diameter, the pressure decreases.

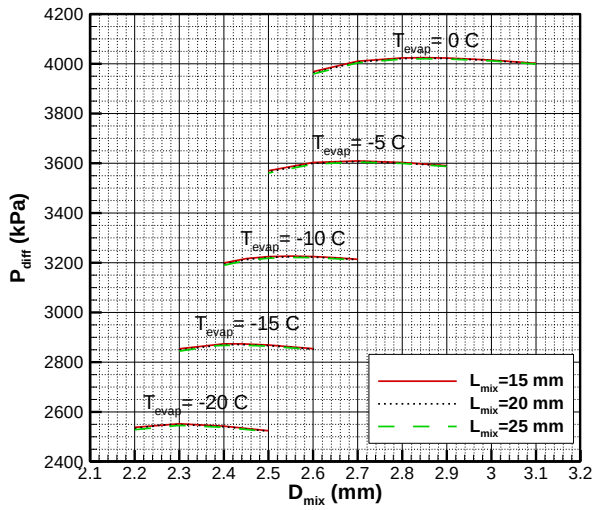

Fig. 18 Variation of ejector pressure outlet with D_{mix} and L_{mix} for different T_{evap}

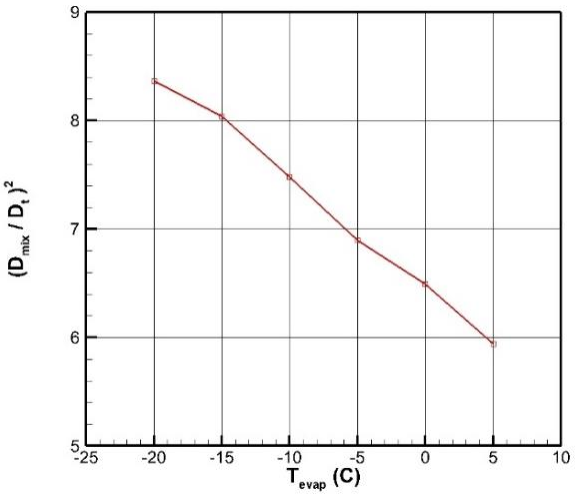

Fig. 19 Variation of $(D_{mix}/D_t)^2$ with different T_{evap}

Probably this variation can be explained by the impact of D_{mix} on the inlet conditions of the diffuser. Due to the low viscosity of CO_2, a limited pressure reduction due to friction forces with the increase of D_{mix} is expected but the influence of velocity change may be more important. The flow at the diffuser inlet presents a diminution of the velocity as well as some increase of the pressure. These two variations have an opposite effect on the role of the diffuser in transforming the residual kinetic velocity into pressure. Probably, the effect that allows to increase the P_{diff} prevails up to the optimal D_{mix}, beyond this diameter the diminution of the velocity tends to negatively impact the pressure recovery of the diffuser which becomes less efficient. Note that the three tested L_{mix} present the same optimal mixing diameter (D_{mix}=2.87 mm) which corresponds to the maximum outlet pressure.

Figure 18 illustrates the effects of D_{mix} on P_{diff} for different evaporator temperatures. For each T_{evap}, there is an optimal D_{mix} that corresponds to a maximum P_{diff}. Overall, a decrease of D_{mix} is observed with T_{evap} due to the diminution of the evaporator capacity.

Figure 19 show the ratio $(D_{mix}/D_t)^2$ assessed with optimal D_{mix} at different T_{evap}. This ratio varies in the range of 6-8.5, which is in line with values found in the literature (Table 3).

Note that the variation of L_{mix} does not generate an optimum on the pressure at the ejector outlet or on any other variable. Thus, the condition used to stop the iterations on L_{mix} is based on data from the literature related to the value of (L_{mix}/D_{mix}) ratio which should be between 6 and 10 (see Table 3). For example, in the case of T_{evap}=0 ºC, L_{mix}=25 mm is selected which correspond to an appropriate L_{mix}/D_{mix}.

Diffuser diameter

Figure 20 shows an example of the diffuser outlet diameter (D_{diff}) calculations; under the condition of T_{evap}=0 ºC and with the mixing geometry of D_{mix}=2.87 mm and L_{mix}=25 mm.

An increase in diffuser diameter leads to a rise in the pressure at the ejector outlet, while the outlet velocity

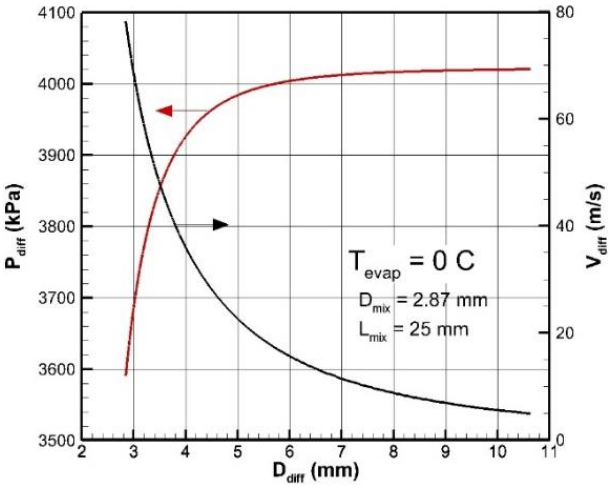

Fig. 20 Variation of pressure and velocity at ejector outlet with D_{diff}

obviously evolves inversely to pressure. Note, that for the diffuser diameter larger than 6 mm, pressure variation is low, reaching a plateau condition. Indeed, from this location to the outlet of the ejector (D_{diff}=10.6 mm), the increase in pressure is less than 0.4%. With a diffuser angle of 5°, considering an outlet diameter of 6 mm instead of 10.6 mm will result in 2.6 times shorter diffuser length; however, with shorter diffuser, outlet velocity is 3 times higher. The selection of the diffuser outlet diameter should be done on the pressure plateau, with a compromise between the outlet velocity and the length of the diffuser.

5. CONCLUSION

First, the benefit of integrating a transcritical CO_2 ejector as an expansion device in a heat pump is shown. The recovered work by the ejector contributes to enhance the compressor operation. At the lower evaporator temperature considered (T_{evap}=-20 ºC), the compressor suction temperature is raised by nearly 5 ºC with a decrease of the optimal gas cooler pressure around 2 bars. Thus, the compression ratio is reduced and the compressor shutdown in cold weather conditions could also be delayed due to higher suction temperature.

Finding the appropriate geometry of the ejector is essential in the use of such systems. The development of a relatively simple and robust model to design transcritical CO_2 two-phase ejectors can address this concern.

The proposed model is built on a thermodynamic HEM approach coupled with NIST-REFPROP equations for thermophysical properties. Nozzles are considered choked. For the motive flow, the mass flux maximization technique is applied. For the secondary nozzle, a fixed Mach number is achieved by adjusting the mass flux. Modeling the mixing process is considered in two steps with variable pressure. Part of the mixing begins in the convergent zone; further mixing then occurs in the constant cross-section zone where wall friction is also considered. The diffuser is designed using an isentropic efficiency and imposing a velocity at the ejector outlet.

A single set of isentropic efficiencies was found and adjusted for a wide range of operational conditions. The model validation with experimental data from the literature is satisfactory. The primary nozzle throat diameter calculations do not exceed an error of ±8% under transcritical conditions. The error on the ejector outlet pressure is in the limit of -15% to +3%.

Finally, a practical use of the ejector design model in combination with experimental data from the literature to compensate some shortcomings of the theoretical approach is presented. The example shows the details for estimating the ejector geometry for a transcritical CO_2 heat pump application under different heat source conditions. The results show the important decrease of primary nozzle diameters with the drop of T_{evap}, especially for the throat. A decrease of D_{mix} also occurs with T_{evap} and an optimal diameter is obtained for each condition considered. The design of the diffuser is based on a compromise between the outlet velocity and the length of the diffuser.

The model and the design approach presented are relatively rapid to implement and to produce results. They are thus well suited for pre-design purposes. For detailed analysis and design refinement, a CFD approach is more appropriate. The next step will be to improve the ejector design by the CFD approach and to run experimental tests with a dedicated test bench.

ACKNOWLEDGEMENTS

Financial support is provided by PERD, a program of Natural Resources Canada for R-D.

CONFLICT OF INTEREST

The authors have no conflicts to disclose.

AUTHORS CONTRIBUTION

K. Ameur: Conceptualization, Methodology, Visualization, Writing. **Z. Aidoun:** Methodology, Writing-Review.

REFERENCES

Aakenes, F. (2012). *Frictional pressure-drop models for steady-state and transient two-phase flow of carbon dioxide*. [Master's thesis, Norwegian University of Science and Technology].

Aidoun, Z., Ameur, K., Falsafioon, M., & Badache, M. (2019a). Current advances in ejector modeling, experimentation and applications for refrigeration and heat pumps. Part 2: Two-phase ejectors. *Inventions*, 4, 1–54. https://doi.org/10.3390/inventions4010016

Aidoun, Z., Ameur, K., Falsafioon, M., & Badache, M. (2019b). Current advances in ejector modeling, experimentation and applications for refrigeration and heat pumps. Part 1: Single-phase ejectors. *Inventions*, 4, 1–73. https://doi.org/10.3390/inventions4010016

Akagi, S., Dang, C., & Hihara, E. (2008). *Characteristics of pressure recovery in two-phase ejector applied to carbon dioxide heat pump cycle*. 9th International IEA Heat Pump Conference, Zürich, Switzerland.

Akagi, S., Wang, J., & Hihara, E., 2004. *Characteristics of two-phase ejector with carbon dioxide*. 41st National Heat Transfer Symposium of Japan.

Ameur, K., & Aidoun, Z. (2021). Two-phase ejector enhanced carbon dioxide transcritical heat pump for cold climate. *Energy Conversion and Management*, 243, 114421. https://doi.org/10.1016/j.enconman.2021.114421

Ameur, K., Aidoun, Z., & Ouzzane, M. (2016). Modeling and numerical approach for the design and operation of two-phase ejectors. *Applied Thermal Engineering* 109, 809–818. https://doi.org/10.1016/j.applthermaleng.2014.11.022

Austin, B. T., & Sumathy, K. (2011). Transcritical carbon dioxide heat pump systems: A review. *Renewable and Sustainable Energy Reviews* 15, 4013–4029. https://doi.org/10.1016/j.rser.2011.07.021

Banasiak, K., & Hafner, A. (2011). 1D Computational model of a two-phase R744 ejector for expansion work recovery. *International Journal of Thermal Sciences* 50, 2235–2247. https://doi.org/10.1016/j.ijthermalsci.2011.06.007

Banasiak, K., & Hafner, A. (2013). Mathematical modelling of supersonic two-phase R744 flows through converging-diverging nozzles : The effects of phase transition models. *Applied Thermal Engineering* 51, 635–643. https://doi.org/10.1016/j.applthermaleng.2012.10.005

Banasiak, K., Hafner, A., & Andresen, T. (2012). Experimental and numerical investigation of the influence of the two-phase ejector geometry on the performance of the R744 heat pump. *International Journal of Refrigeration 35*, 1617–1625. https://doi.org/10.1016/j.ijrefrig.2012.04.012

Banasiak, K., Hafner, A., Kriezi, E. E., Madsen, K. B., Birkelund, M., Fredslund, K., & Olsson, R. (2015). Development and performance mapping of a multi-ejector expansion work recovery pack for R744 vapour compression units. *International Journal of Refrigeration* 57, 265–276. https://doi.org/10.1016/j.ijrefrig.2015.05.016

Banasiak, K., Palacz, M., Hafner, A., Bulinski, Z., Smołka, J., Nowak, A. J., & Fic, A. (2014). A CFD-based investigation of the energy performance of two-phase R744 ejectors to recover the expansion work in refrigeration systems : An irreversibility analysis. *International Journal of Refrigeration* 40, 328–337. https://doi.org/10.1016/j.ijrefrig.2013.12.002

Besagni, G., Mereu, R., & Inzoli, F. (2016). Ejector refrigeration: A comprehensive review. *Renewable and Sustainable Energy Reviews* 53, 373–407. https://doi.org/https://doi.org/10.1016/j.rser.2015.08.059

Bouziane, A., Bensafi, A., & Haberschill, P. (2012). *Modeling and experimental study of an ejector for a transcritical co2 refrigeration system.* 10 Th IIR Gustav Lorentzen Conference on Natural Refrigerants. Delft, The Netherlands.

Cardemil, J., & Colle, S. 2011. *Novel cascade ejector cycle using natural refrigerants*. 23rd IIR International Congress of Refrigeration. Prague, Czech Republic.

Eames, I., Aphornratana, S., & Haider, H. (1995). A theoretical and experimental study of a small-scale steam jet refrigerator. *International Journal of Refrigeration* 18, 378–386. https://doi.org/10.1016/0140-7007(95)98160-M

Elbel, S. (2011). Historical and present developments of ejector refrigeration systems with emphasis on transcritical carbon dioxide air-conditioning applications. *International Journal of Refrigeration* 34, 1545–1561. https://doi.org/10.1016/j.ijrefrig.2010.11.011

Elbel, S., & Hrnjak, P. (2008). Experimental validation of a prototype ejector designed to reduce throttling losses encountered in transcritical R744 system operation. *International Journal of Refrigeration* 31, 411–422. https://doi.org/10.1016/j.ijrefrig.2007.07.013

Environment and Climate Change Canada (2022) Canadian Environmental Sustainability Indicators: Greenhouse gas emissions. Gatineau, Canada.

Giacomelli, F., Mazzelli, F., Banasiak, K., Hafner, A., & Milazzo, A. (2019). Experimental and computational analysis of a R744 flashing ejector. *International Journal of Refrigeration* 107, 326–343. https://doi.org/10.1016/j.ijrefrig.2019.08.007

Henry, R. E., & Fauske, H. K. (1971). The two-phase critical flow of one-component mixtures in nozzles, orifice, and short tubes. *Journal of Heat Transfer*, 93, 179–187. https://doi.org/10.1115/1.3449782

Huff, H. J., & Radermacher, R. (2003). *CO2 compressor-expander analysis.* ARTI-21CR/611-10060-01. Arlington.

Kornhauser, A. A. (1990). *The Use of an ejector as a refrigerant expander.* International Refrigeration and Air Conditioning Conference. Purdue University. Paper 82.

Lee, J. S., Kim, M. S. Kim, & M. S. Kim (2011). Experimental study on the improvement of CO2 air conditioning system performance using an ejector. *International Journal of Refrigeration* 34, 1614–1625. https://doi.org/10.1016/j.ijrefrig.2010.07.025

Li, D., & Groll, E. A. (2006). *Analysis of an ejector expansion device in a transcritical CO2 air conditioning system.* 7th IIR Gustav Lorentzen Conference on Natural Working Fluids. Trondheim, Norway.

Liu, F., Groll, E. A., & Li, D. (2012a). Investigation on performance of variable geometry ejectors for CO2 refrigeration cycles. *Energy*, 45, 829–839. https://doi.org/10.1016/j.energy.2012.07.008

Liu, F., Li, Y., & Groll, E. A. (2012b). Performance enhancement of CO2 air conditioner with a controllable ejector. *International Journal of Refrigeration* 35, 1604–1616. https://doi.org/10.1016/j.ijrefrig.2012.05.005

Lucas, C., & Koehler, J. (2012). Experimental investigation of the COP improvement of a refrigeration cycle by use of an ejector. *International Journal of Refrigeration* 35, 1595–1603. https://doi.org/10.1016/j.ijrefrig.2012.05.010

Ma, Y., Liu, Z., & Tian, H. (2013). A review of transcritical carbon dioxide heat pump and refrigeration cycles. *Energy*, 55, 156–172. https://doi.org/10.1016/j.energy.2013.03.030

Mastrowski, M., Smolka, J., Hafner, A., Haida, M., Palacz, M., & Banasiak, K. (2019). Experimental study of the heat transfer problem in expansion devices in CO2 refrigeration systems. *Energy*, 173, 586–597. https://doi.org/10.1016/j.energy.2019.02.097

Minetto, S., Brignoli, R., Banasiak, K., Hafner, A., & Tesser, F. (2012). *Experimental analysis of a r744 heat pump equipped with an ejector*. The 10 Th IIR Gustav Lorentzen Conference on Natural Refrigerants. Delft, The Netherlands.

Nakagawa, M., Marasigan, A. R., Matsukawa, T., & Kurashina, A. (2011). Experimental investigation on the effect of mixing length on the performance of two-phase ejector for CO2 refrigeration cycle with and without heat exchanger. *International Journal of Refrigeration* 34, 1604–1613. https://doi.org/10.1016/j.ijrefrig.2010.07.021

NIST (2010). *NIST thermodynamics and transport properties of refrigerants and refrigerant mixtures-REFPROP* (Version 9.0).

Palacz, M., Haida, M., Smolka, J., Nowak, A. J., Banasiak, K., & Hafner, A. (2017). HEM and HRM accuracy comparison for the simulation of CO2 expansion in two-phase ejectors for supermarket refrigeration systems. *Applied Thermal Engineering* 115, 160–169. https://doi.org/10.1016/j.applthermaleng.2016.12.122

Ringstad, K. E., Allouche, Y., Gullo, P., Ervik, Å., Banasiak, K., & Hafner, A. (2020). A detailed review on CO2 two-phase ejector flow modeling. *Thermal Science and Engineering Progress* 20. https://doi.org/10.1016/j.tsep.2020.100647

Rony, R. U., Yang, H., Krishnan, S., & Song, J. (2019). Recent advances in transcritical CO2 (R744) heat pump system: A review. *Energies*, 12, 1–35. https://doi.org/10.3390/en12030457

Saeed, M. Z., Hafner, A., Thatte, A., & Gabrielii, C. H. (2022, June 13-15). *Simultaneous implementation of rotary pressure exchanger and ejectors for CO2 refrigeration system*. 15th IIR-Gustav Lorentzen Conference on Natural Refrigerants. Trondheim, Norway.

Sarkar, J. (2010). Review on cycle modifications of transcritical CO2 refrigeration and heat pump systems. *Journal of Advanced Research in Mechanical Engineering* 1, 22–29.

Smolka, J., Bulinski, Z., Fic, A., Nowak, A. J., Banasiak, K., & Hafner, A. (2013). A computational model of a transcritical R744 ejector based on a homogeneous real fluid approach. *Applied Mathematical Modelling* 37(3), 1208–1224. https://doi.org/10.1016/j.apm.2012.03.044

Takleh, H. R., & Zare, V. (2019). Performance improvement of ejector expansion refrigeration cycles employing a booster compressor using different refrigerants: Thermodynamic analysis and optimization. *International Journal of Refrigeration* 101, 56–70. https://doi.org/10.1016/j.ijrefrig.2019.02.031

Taslimi Taleghani, S., Sorin, M., & Poncet, S. (2018). Modeling of two-phase transcritical CO2 ejectors for on-design and off-design conditions. *International Journal of Refrigeration* 87, 91–105. https://doi.org/10.1016/j.ijrefrig.2017.10.025

Zha, S., Jakobsen, A., Hafner, A., & Neksa, P. (2007). *Design and parametric investigation on ejector for R-744 transcritical system*. International Congress of Refrigeration 2007. Beijing.

Zhu, Y., & Jiang, P. (2018). Theoretical model of transcritical CO2 ejector with non-equilibrium phase change correlation. *International Journal of Refrigeration* 86, 218–227. https://doi.org/10.1016/j.ijrefrig.2017.10.033

Zhu, Y., Li, C., Zhang, F., & Jiang, P. X. (2017). Comprehensive experimental study on a transcritical CO2 ejector-expansion refrigeration system. *Energy Conversion and Management* 151, 98–106. https://doi.org/10.1016/j.enconman.2017.08.061